Astronomy & Astrophysics manuscript no. Irregular-occ
August 4, 2015

Predictions of stellar occultations of 9 irregular satellites of giant planets

A. R. Gomes-Júnior[1], M. Assafin[1,⋆], R. Vieira-Martins[1,2,3,⋆⋆], J. I. B. Camargo[2,3], B. E. Morgado[1],

[1] Observatório do Valongo/UFRJ, Ladeira Pedro Antônio 43, CEP 20.080-090 Rio de Janeiro - RJ, Brazil
e-mail: altair08@astro.ufrj.br
[2] Observatório Nacional/MCT, R. General José Cristino 77, CEP 20921-400 Rio de Janeiro - RJ, Brazil
e-mail: rvm@on.br
[3] Laboratório Interinstitucional de e-Astronomia - LIneA, Rua Gal. José Cristino 77, Rio de Janeiro, RJ 20921-400, Brazil

Received ; accepted

ABSTRACT

Key words. Occultations - Planets and satellites: general - Planets and satellites: individual: Jovian and Saturnian irregular satellites

1. Introduction

Irregular satellites, also known as outer satellites, of the giant planets are objects orbiting the planets from a distant, eccentric and highly inclined orbit, most of them are retrograde. Because of these peculiar orbits, it is largely accepted that these objects were captured by their planets in the early solar system (Sheppard 2005).

There is a number of capture mechanisms of objects by giant planets proposed in the literature. There is the Gas Drag in the primordial circumplanetary nebulae (Sheppard 2005) where the object would be affected by the gas drag and its velocity slowed down until it be captured by the planet. Another mechanism is called pull-down capture (Sheppard 2005), where the mass of the planet would increase while the object was temporarily captured.

A mechanism based in the Nice model (Morbidelli et al. 2005; Tsiganis et al. 2005; Gomes et al. 2005) was proposed by Nesvorný et al. (2007) and, in the specific case of Jupiter with the modern Nice model, by Nesvorný et al. 2014. During the early solar system instability, encounters between the outer planets occurred. These planetary encounters could exchange energy and angular momentum between planets and the objects nearby making it possible for the capture of irregular bodies by the giant planets. In this scenario, the survival rate of prior-LHB (Late Heavy Bombardment) satellites is very small.

Another important mechanism is the capture through collisional interactions (Sheppard 2005). A collision between two small bodies in the Hill's sphere of the planet could generate fragmented objects and the dissipated energy could be such that some of these objects could be captured.

Some of these objects are in dynamical groups with similar orbital elements, called families, similar to families found in the Main Asteroid Belt. These families may have been created by a parent body disrupted by collisions with comets or other satellites (Nesvorný et al. 2004). Collisions with comets are more likely to have occurred during the ~~Late Heavy Bombardment (LHB)~~ (Gomes et al. 2005).

Nesvorný et al. (2003) studied the collision rates between irregular satellites and concluded that some satellites could have been removed by collision with a bigger satellite. The rate collision between satellites of the Himalia Group (Himalia, Elara, Lysithea and Leda, mainly), for instance, was found to be more than one during the solar system age suggesting that their current structure was originated by satellite-satellite collision.

For Phoebe, ejected material from its surface caused by impacts could evolve due to Poynting-Robertson drag and collide with Iapetus causing the large variation in albedo observed on it (Nesvorný et al. 2003). Indeed, Cassini was able to detected in Phoebe an absorption feature at 2.42 μm (probably CN combinations) that was also detected in the dark side of Iapetus (Clark et al. 2005).

The region of origin of the ject is not well known, Grav et al. (2003) and Grav & Bauer (2007) showed that the irregular satellites from the giant planest have their colors and spectral slopes similar to C-, D- and P-type asteroids, Centaurs and trans-neptunian objects (TNOs) suggesting that they have been originated from d nt locations in the early solar system.

In this work, we stu these ob as possible representatives o small TNOs population. TNOs are obje at due to their distance may be highly preserved having their properties similar to those they had when they were formed, then providing histor d evolution of the outer solar system (Camargo et al. 2013). Due to their distance, the smaller objects from this region are more difficult to observe and study.

In the intent to obtain the physical parameters (size, shape, albedo, density, etc) of the irregular satellites and help identify their origin locations, we will make use of the stellar occultation technique. This technique is the best one to obtain these parameters of the solar system objects from ground-based observations providing more accurate results than other ground-based techniques (Sicardy et al. 2011; Ortiz et al. 2012; Braga-Ribas et al. 2014).

Send offprint requests to: A. R. Gomes-Júnior
⋆ Affiliated researcher at Observatoire de Paris/IMCCE, 77 Avenue Denfert Rochereau 75014 Paris, France
⋆⋆ Affiliated researcher at Observatoire de Paris/IMCCE, 77 Avenue Denfert Rochereau 75014 Paris, France

Since their estimated sizes are very small (see Table **??** Ainda vou fazer a tabela), predict the exact location and instant where the shadow will cross the Earth demands a good precision. For instance, the bigger irregular satellite of Jupiter has an estimated size of 186 km (Porco 2003), which is equivalent to an apparent size of 40 mas, must have an error smaller than its size for being observable. For the other objects, smaller or farther than Himalia, the situation is more difficult.

As pointed out by Gomes-Júnior et al. (2015), the ephemeris of the irregular satellites have errors that may reach 200 mas for some satellites. For an object at the distance of Jupiter represents an error bigger than 700 km in the shadow path.

We present in this paper the stellar occultation predictions for the 7 major irregular satellites of Jupiter (Himalia, Elara, Pasiphae, Lysithea, Carme, Ananke and Sinope), Phoebe from Saturn and Triton and Nereid from Neptune. In the section 2 we explore the scientific rationale for study the irregular satellites and the possibility of having a common origin with TNOs. In section 3 we show the correction made to the ephemeris for better predict stellar occultations. In section 4, we present the predictions of the stellar occultations by irregular satellites and how they were made. Some test realized to confirm the predictions are presented in section 5 and the conclusion is given in section 6.

2. Scientific Rationale

As explicited in section 1, there is no consensus on a single model about the region where the irregular satellites were formed. In this work we treat them as having a common origin to the Centaurs and TNOs. In this case, they would be the representative objects of the small TNOs population. Since that small objects at great distances are difficult to study, the irregular satellites can complement this gap.

3. Correction of the ephemeris

Gomes-Júnior et al. (2015) showed from observations made at the Observatório do Pico dos Dias (OPD), Observatoire Haute Provence (OHP) and European Southern Observatory (ESO) that the orbits of the irregular satellites of the giant planets have systematic errors. The offsets of the observations relative to the JPL ephemeris could be up to 200 mas for some satellites. These differences could be associated with errors in their orbital elements.

Making a new model for the orbits of these objects would demand a lot of time and delay the publication of these predictions. Then we utilize the offsets obtained by Gomes-Júnior et al. (2015) to identify a pattern in the error of the ephemeris. This pattern could be used to extrapolate an offset to the satellite ephemeris by the time of the occultation predicted. Plots of the offsets over time and true anomaly (see Fig. 3 and 3 for Carme) clearly show the systematic error in the JPL ephemeris.

$$F(t, f) = p[0] \times t + p[1] \times \sin(f) + p[2] \times \cos(f) + p[3], \quad (1)$$

$$F(t, f) = p[0] \times \sin\left(\frac{2\pi}{p[1]} \times t + p[2]\right) + p[3] \times \sin(f) + \\ + p[4] \times \cos(f) + p[5], \quad (2)$$

where $F(t, f)$ is the offset obtained, t is time in years counting from J2000.0 and f is the true anomaly.

Falta justificar as funções

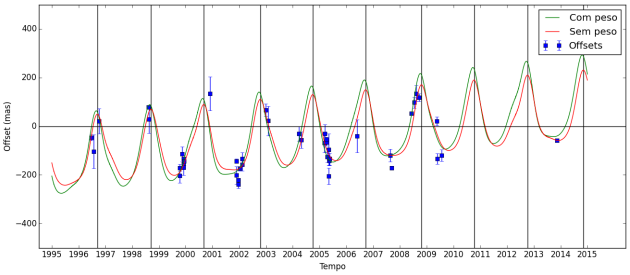

Fig. 1. Offsets of the declination of Carme by time. Figura só para visualização, vou colocar alguma melhor depois

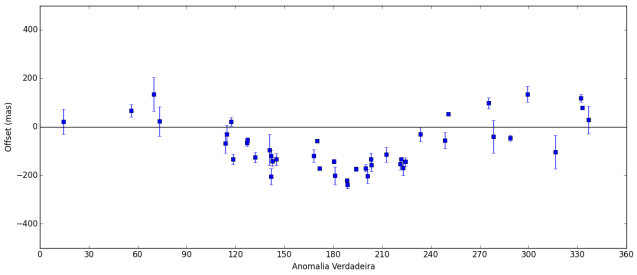

Fig. 2. Offsets of the declination of Carme by true anomaly. Figura só para visualização, vou colocar alguma melhor depois

4. Prediction of occultations

The prediction of the occultations was made by crossing the stellar coordinates and proper motions of the UCAC4 catalogue (Zacharias et al. 2013) with the corrected JPL ephemeris as presented in the section 3. The search for stellar candidates follows the same procedure as presented by Assafin et al. (2010, 2012) and Camargo et al. (2013).

It was predicted occultation by the 7 major irregular satellites of Jupiter, Phoebe of Saturn and Triton and Nereid of Neptune.

For Triton and Nereid, the candidates for stellar occultations in 2015 and 2016 was searched using the WFI catalogue in the same way as the predictions for Centaurs and TNOs occultations by Assafin et al. (2010, 2012) and Camargo et al. (2013). This catalogue contains the stars in the path of Neptune in the sky up to mid-2016. The catalogue was generated by observations made at the ESO 2p2 telescope (IAU code 809) using the Wide Field Imager (WFI) CCD mosaic detector. The filter used was the broad-band R filter ESO#844 with λ_c = 651.725 nm and $\Delta\lambda$ = 162.184 nm.

A total of 588 events (Não estou contando ainda os eventos para Tritão) were identified between January 2015 and December 2017. Table 1 exemplifies the catalogue of occultations generated and their parameters, which is necessary to produce occultation maps (see Fig. 3 as an example). Since these objects are very small, the duration of each event is a few seconds.

5. Occultation tests

Observe a stellar occultation by an irregular satellites demands a great effort. The shadow covers a very restricted area on Earth because the irregular satellites are small. So before we start a large observational campaign, we tested some occultation predictions for larger objects, to assess the quality of the prediction.

This test consists in observing the object and star to be occulted near the event when the two objects are projected in the same field of view, preferably when the objects are close to each other. Thus the relative positions between the two objects will

Table 1. Extract of prediction table. Ainda tenho que fazer a tabela melhor, encaixar. Abaixo é um exemplo apenas para visualização.

d m Year	h m s	RA (ICRS)	Dec	C/A	P/A	v	D	R*	λ	LST	$\Delta e_{\alpha*}$	Δe_{δ}	pm
07 10 2015	21 52 34.	10 53 40.1835	+08 21 00.489	0.465	200.31	39.31	6.25	16.6	179.	09:48	-31.0	-13.0	ok
23 10 2015	07 54 50.	11 05 26.6037	+07 14 32.030	1.017	201.33	36.11	6.12	15.5	16.	08:59	-31.0	-13.0	ok
31 10 2015	00 24 19.	11 10 56.2964	+06 42 07.110	1.801	21.84	33.94	6.04	16.9	123.	08:34	-31.0	-13.0	ok
07 11 2015	1 22 53.	11 16 14.3041	+06 10 05.194	0.306	202.36	31.33	5.94	16.2	162.	08:09	-31.0	-13.0	ok
08 11 2015	04 27 21.	11 16 25.7881	+06 08 55.566	1.077	202.38	31.23	5.94	16.9	55.	08:08	-31.0	-13.0	ok

Notes. Occultation table: day of the year and UTC time of the prediction; right ascension and declination of the occulted star - in the original table, these coordinates are immediately followed by the geocentric astrometric equatorial coordinates (corrected for the offset or ephemeris method), not presented here, of the occulting body; C/A: the geocentric closest approach, in arcseconds; P/A: the planet position angle with respect to the occulted star at C/A, in degrees; velocity in plane of sky, in km s^{-1}: positive = prograde, negative = retrograde; D: planet range to Earth, in AU; R*: normalized magnitude to a common shadow velocity of 20 km s^{-1} by the relationship $\mathrm{Mag}* = \mathrm{Mag}_{\mathrm{actual}} + 2.5 \times \log 10\left(\frac{\mathrm{velocity}}{20\mathrm{km\,s^{-1}}}\right)$. A value of 50.0 means that the star is not in the 2MASS; λ: east longitude of subplanet point in degrees, positive towards east; LST: UT + λ: local solar time at subplanet point, hh:mm; $\Delta e_{\alpha*}$ and Δe_{δ}: offset in mas applied to the ephemeris right ascension and declination, respectively; pm: ok = proper motion applied, no = no proper motion applied; catalogue cross-identification (ct) = uc (UCAC2), 2m (2MASS), fs (field star); f = multiplicity flag (see Table 3); $E_{\alpha*}$ and E_{δ}: uncertainties (mas) in right ascension and declination. A value of 9999 means that there was no estimation of the respective uncertainty; $\mu_{\alpha*}$ and μ_{δ}: proper motions in right ascension and declination, respectively (mas/year).

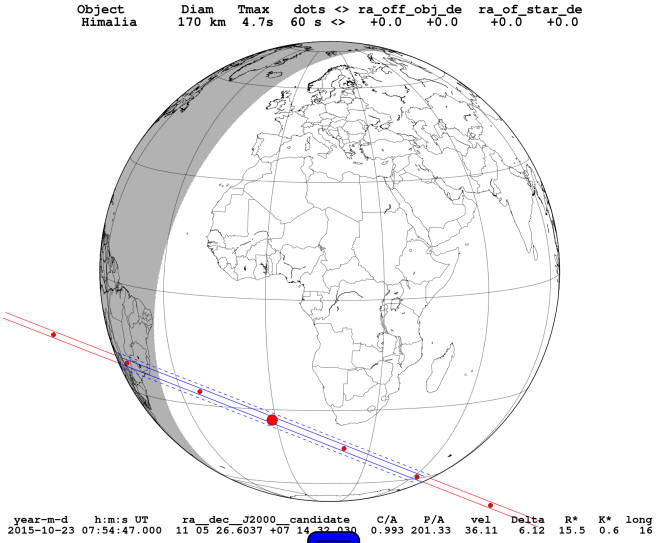

Fig. 3. Occultation map for Himalia Mapa de Himalia para exemplificar, posso colocar outro depois. Compare the information given in caption with the second entry of Table 1

Table 2. Comparison between the predictions of Himalia. Ainda vou terminar de preencher a tabela e tem que ver direito o offset do ajuste

Difference from nominal prediction		
Method	Instant of C/A	C/A
Nominal	2015-03-03 00:39:25 UT	0.714″
Offset	-07 s	
Feb. 22 Obs.	+15 s	
Mar. 03 Obs.	-10 s	

have minimal influence of the errors of the catalogue of stars used and possible field distortions (Peng et al. 2008, and references therein). The offsets of the positions of the star and the satellites will be used to correct the predictions.

To date, two occultation tests were performed, one by Himalia that occurred on March 3, 2015 and the second by Elara that occurred on March 30, 2015. For each event, four maps were generated: the first with the nominal positions of the star and the satellite to the predicted time; the second with the offset calculated as described in section 3; the third with star and satellite offsets from observations made a few days before the occultation when the two objects were separated (different FOV); and the fourth from observations made when the star and the satellite were close in the same FOV.

Figure 4. Shows the four maps for Himalia occultation test in March 03, 2015. The map 4a is the nominal prediction with the coordinate of the star given by the catalogue and that of the satellite from the ephemeris. We then corrected the positions of the satellite by an offset calculated by the method showed in section 3 to make the map 4b.

The map 4c was made from obtained positions on February 22 observed with the Zeiss telescope at the Observatório do Pico dos Dias (OPD). On that day, Himalia and the star were observed in separate FOVs as they were still far apart. On the night of the event, March 3, the objects were observed with Perkin-Elmer telescope at OPD just over an hour after the time scheduled for the event. Satellite and star were separated by about 16 arcsec, so very close to each other. From the calculated offsets, the map 4d was generated.

In this event, it is possible to see that the shade does not vary much among the four maps suggesting that, at least for Himalia, there is a greater probability of observing an event. In fact, the biggest difference between the shadows of the four maps are 25s and 130km in the direction perpendicular to the shadows (see table 2).

The second test was with the satellite Elara, which is the second biggest irregular satellites of Jupiter. The event was predict the occur at March 30, 2015. The observations were taken on March 25 and April 2, 2015 with the Zeiss telescope. On the night of April 2 they could still be observed in the same FOV. Due to Elara be much weaker, dispersions of the satellite positions on both nights ended up being higher than for Himalia. Still, the differences between the maps obtained were relatively small. The biggest difference between them is 73s and 302km (see table 3).

6. Conclusion

Acknowledgements. ARG-J thanks the financial support of CAPES. MA thanks the CNPq (Grants 473002/2013-2 and 308721/2011-0) and FAPERJ (Grant E-

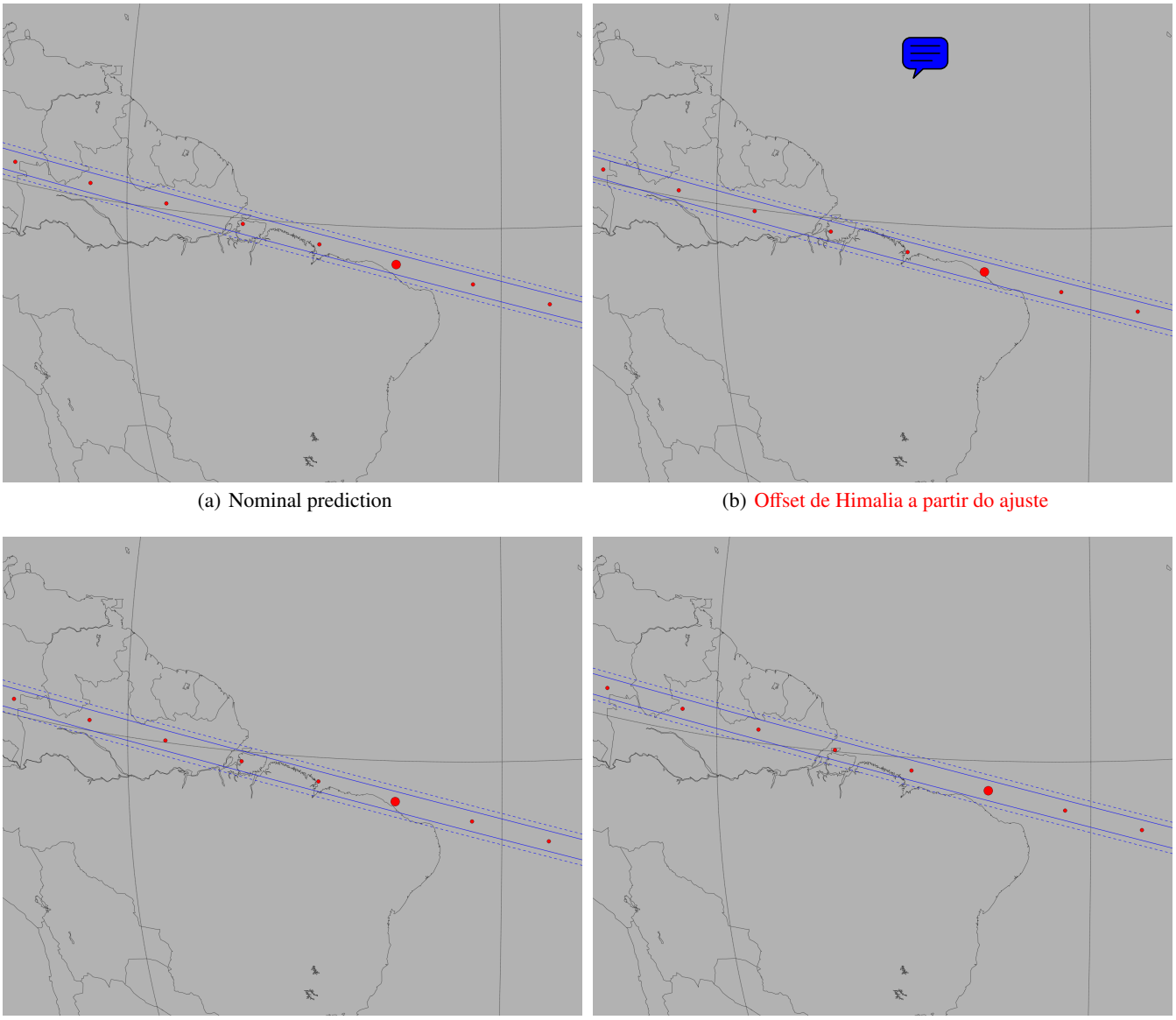

(a) Nominal prediction

(b) Offset de Himalia a partir do ajuste

(c) Observation at February 22 (different FOVs)

(d) Observation at March 03 (same FOV)

Fig. 4. Predictions for Himalia: The big red dot show the geocentric closest approach of the shadow. The small red ones are the center of the shadow separated by one minute. The straight lines show the size of the shadow. 4a is the map using the nominal positions of the star and satellite. 4b shows the shadow given an estimated offset for the position of Himalia related to the JPL ephemeris obtained in section 3. In 4c we apply offsets to the positions of star and satellite accordingly the observations made at February 22. In 4d is as in 4c but with observations made at March 03 when the objects were close to each other. Figuras ainda serão mudadas. Colocadas para visualização

Table 3. Comparison between the predictions of Elara. Ainda vou terminar de preencher a tabela e tem que ver direito o offset do ajuste

Difference from nominal prediction		
Method	Instant of C/A	C/A
Nominal	2015-03-30 01:45:15 UT	1.139″
Offset	-16 s	
Mar. 25 Obs.	-58 s	
Apr. 02 Obs.	+15 s	

26/111.488/2013). RV-M thanks grants: CNPq-306885/2013, Capes/Cofecub-2506/2015, Faperj/PAPDRJ-45/2013. JIBC acknowledges CNPq for a PQ2 fellowship (process number 308489/2013-6). FB-R acknowledges PAPDRJ-FAPERJ/CAPES E-43/2013 number 144997, E-26/101.375/2014. BEM thanks the financial support of CAPES.

References

Assafin, M., Camargo, J. I. B., Vieira Martins, R., et al. 2010, Astronomy & Astrophysics, 515, A32
Assafin, M., Camargo, J. I. B., Vieira Martins, R., et al. 2012, Astronomy & Astrophysics, 541, A142
Braga-Ribas, F., Sicardy, B., Ortiz, J. L., et al. 2014, Nature, 508, 72–75
Camargo, J. I. B., Vieira-Martins, R., Assafin, M., et al. 2013, Astronomy & Astrophysics, 561, A37
Clark, R. N., Brown, R. H., Jaumann, R., et al. 2005, Nature, 435, 66–69
Gomes, R., Levison, H. F., Tsiganis, K., & Morbidelli, A. 2005, Nature, 435, 466–469
Gomes-Júnior, A. R., Assafin, M., Vieira-Martins, R., et al. 2015, Astronomy & Astrophysics
Grav, T. & Bauer, J. 2007, Icarus, 191, 267–285
Grav, T., Holman, M. J., Gladman, B. J., & Aksnes, K. 2003, Icarus, 166, 33–45
Morbidelli, A., Levison, H. F., Tsiganis, K., & Gomes, R. 2005, Nature, 435, 462–465
Nesvorný, D., Alvarellos, J. L. A., Dones, L., & Levison, H. F. 2003, AJ, 126, 398–429

Nesvorný, D., Beaugé, C., & Dones, L. 2004, AJ, 127, 1768–1783
Nesvorný, D., Vokrouhlický, D., & Deienno, R. 2014, ApJ, 784, 22
Nesvorný, D., Vokrouhlický, D., & Morbidelli, A. 2007, AJ, 133, 1962–1976
Ortiz, J. L., Sicardy, B., Braga-Ribas, F., et al. 2012, Nature, 491, 566–569
Peng, Q., Vienne, A., Lainey, V., & Noyelles, B. 2008, Planetary and Space Science, 56, 1807–1811
Porco, C. C. 2003, Science, 299, 1541–1547
Sheppard, S. S. 2005in (Cambridge University Press (CUP)), 319
Sicardy, B., Ortiz, J. L., Assafin, M., et al. 2011, Nature, 478, 493–496
Tsiganis, K., Gomes, R., Morbidelli, A., & Levison, H. F. 2005, Nature, 435, 459–461
Zacharias, N., Finch, C. T., Girard, T. M., et al. 2013, The Astronomical Journal, 145, 44